Arctic and Antarctic diurnal and seasonal variations of snow albedo from multiyear Baseline Surface Radiation Network measurements

Xianwei Wang[1,2] and Charles S. Zender[2]

Received 26 August 2010; revised 18 April 2011; accepted 6 May 2011; published 6 August 2011.

[1] This study analyzes diurnal and seasonal variations of snow albedo at four Baseline Surface Radiation Network stations in the Arctic and Antarctica from 2003 to 2008 to elucidate similarities and differences in snow albedo diurnal cycles across geographic zones and to assess how diurnal changes in snow albedo affect the surface energy budget. At the seasonal scale, the daily albedo for the perennial snow at stations South Pole and Georg von Neumayer in Antarctica has a similar symmetric variation with solar zenith angle (SZA) around the austral summer; whereas the daily albedo for the seasonal snow at stations Barrow, Alaska, and Ny-Ålesund, Spitsbergen, in the Arctic tends to decrease with SZA decrease from winter to spring before snow starts melting. At the hourly scale, each station shows unique diurnal cycles due to different processes that affect snow albedo such as cloud cover, snow metamorphism, surface hoar formation, SZA, solar azimuth angle, and surface features. Cloud escalates the snow albedo at all four stations by shifting solar radiation to visible wavelengths and diminishes the diurnal variation by diffusing incident solar radiation. The 24 h mean snow albedo is higher on cloudy than clear days by 0.02 at the South Pole (December) and Barrow (May), 0.05 at Neumayer (December), and 0.07 at Ny-Ålesund (April). Snow surface structures, for example, wind-channeled sastrugi, appear to be a controlling factor in the diurnal variation of clear-sky snow albedo at the South Pole and Ny-Ålesund. The surface hoar formation cycles and snow metamorphism are consistent with the asymmetric diurnal variation of snow albedo at Neumayer and Barrow. Near the melting point temperature, melt-freeze cycles exceed cloud and surface structure impacts and dominate the diurnal variation of snow albedo at stations Barrow and Ny-Ålesund. The satellite-measured clear-sky snow albedo usually underestimates the average all-sky snow albedo at these stations. These results illustrate the potential biases in daily and monthly albedo products constructed from sun-synchronous satellite daily instantaneous observations which inevitably undersample the diurnal variation of snow albedo.

Citation: Wang, X., and C. S. Zender (2011), Arctic and Antarctic diurnal and seasonal variations of snow albedo from multiyear Baseline Surface Radiation Network measurements, *J. Geophys. Res.*, *116*, F03008, doi:10.1029/2010JF001864.

1. Introduction

[2] The shortwave (SW) broadband snow albedo (referred to as snow albedo hereafter) is of great interest to climate studies in that it describes the net solar radiation flux at the snow surface and small errors or changes in its value represent large fractional changes in absorbed solar radiation (ASR) and in the overall heat budget at the snow surface [*Carroll and Fitch*, 1981; *Pirazzini*, 2004]. Although snow albedo dominates the surface energy budget of the Arctic and Antarctica [*Hall*, 2004], the remote location, harsh conditions, extensive cloud cover, and large solar zenith angles in these regions combine to hinder the development of climatological data records of snow albedo. As a result, little is known about the climatological diurnal cycle of polar snow albedo, and its geographic and seasonal variations. Recently, the Baseline Surface Radiation Network (BSRN) has accumulated long time series of high quality, high frequency radiometric data to allow climatological characterization of the diurnal cycle of in situ snow albedo. This study analyzes diurnal and seasonal variations of snow albedo at four BSRN stations in the Arctic and Antarctica from 2003 to 2008 to elucidate similarities and differences in snow albedo cycles in polar regions, to identify physical processes theoretically consistent with these differences, and

[1]School of Geography and Planning and Guangdong Key Laboratory for Urbanization and Geo-Simulation, Sun Yat-sen University, Guangzhou, China.
[2]Department of Earth System Science, University of California, Irvine, California, USA.

0148-0227/11/2010JF001864

to assess how changes in snow albedo affect the surface energy budget.

[3] Snow has high reflectance in visible (VIS) and low reflectance in infrared (IR) wavelengths. Snow bidirectional reflectance varies strongly with solar zenith angle (SZA) and viewing geometry [*Wiscombe and Warren*, 1980; *Salomon et al.*, 2006]. However, climate models typically represent only the zenith, not the azimuthal dependence of snow albedo [*Roesch*, 2006]. Snow directional-hemispherical reflectance has a larger magnitude of increase with SZA in IR (1.03 μm) than in VIS (0.55 μm) wavelengths [*Schaepman-Strub et al.*, 2006]. Snow albedo integrates the angular and spectral variations of snow reflectance over the entire solar spectrum (SW) wavelengths, and has strong diurnal and seasonal cycles depending on both atmospheric and surface conditions [*Pirazzini*, 2004].

[4] Dry snow albedo depends on internal snow characteristics such as snow grain size and shape, snowpack depth, surface roughness, light-absorbing impurities, and on external factors, including the SZA and solar azimuth angle (SAA), the spectral distribution of solar radiation, atmospheric conditions (clouds, water vapor and aerosol, etc.), and shadowing [*Warren*, 1982; *Pirazzini*, 2004]. Observations confirm the predictions of models that, all else being equal, snow albedo increases with decreasing snow grain size and with increasing SZA [*Warren and Wiscombe*, 1980; *Jin et al.*, 2003]. For example, increasing SZA from 0° to 60° increases clear sky snow albedo of a model snowpack from 0.75 to 0.78 [*Wang and Zender*, 2010a]. Falling snow often consists of fine and/or multifaceted snow grains and has higher albedo immediately after snowfall [*Grenfell and Perovich*, 2008]. Doubling the effective radius of ice crystals from 100 to 200 μm, as can occur during a few days of isothermal aging in warm conditions, may reduce albedo from 0.85 to 0.80 [*Taillandier et al.*, 2007].

[5] Cloud cover affects both the spectral distribution of solar irradiance and the effective SZA, resulting in an increase of snow albedo of 0.05–0.1 from its value in clear sky in Antarctica [*Wiscombe and Warren*, 1980; *Pirazzini*, 2004]. Small amounts of strongly absorbing impurities, especially soot, although dust and volcanic ash can also be effective in larger quantities, lower snow albedo mainly in the VIS spectral regions ($\lambda < 0.9$ μm) where absorption by pure snow is weakest. Light-absorbing impurities within snow cause the greatest reductions in albedo for coarse-grained snow [*Warren and Wiscombe*, 1980; *Warren*, 1982]. When the sun azimuth is perpendicular to the long axis of the wind channeled surface features known as sastrugi at the South Pole, snow albedo is reduced as much as 4% from its value when the sun beam is parallel to the sastrugi [*Carroll and Fitch*, 1981].

[6] Snow albedo dynamically changes because of its changing internal properties and external environments. Under overcast skies, surface insolation is diffuse and nearly isotropic, so the effects of SZA and SAA on albedo are negligible, and when snow metamorphism is slow the snow albedo remains rather constant throughout the day [e.g., *Pirazzini*, 2004]. During clear days, snow albedo undergoes large variations due to shadowing, surface hoar, snow metamorphism and changes in SZA and SAA. The diurnal variation (maximum minus minimum) of snow albedo was measured as about 0.04 at the South Pole [*Carroll and Fitch*, 1981], and reaches up to 0.15 on the Antarctic coast [*Pirazzini*, 2004; *Wuttke et al.*, 2006] and over sea ice in the Baltic Sea [*Pirazzini et al.*, 2006]. For a snowpack with mean albedo of 0.8, a diurnal albedo change of 0.10 represents a diurnal ASR change of 50%. This ASR change is significant for climate or surface process models, especially in seasonally snow covered regions where changes in ASR can accelerate the onset of snowmelt and its attendant strong snow albedo feedbacks [*Flanner et al.*, 2007]. For comparison, the diurnal variation of surface albedo in a natural grassland (mean albedo of about 0.2) is 0.05 [*Song*, 1998], and could be up to 0.1 (or a ASR change of 12%) at a given SZA due to the formation of dew and inclined canopies by prevailing wind direction [*Minnis et al.*, 1997].

[7] Despite the numerous mechanisms besides SZA which can contribute to the diurnal cycle of snow albedo, methods for remote sensing of surface properties, estimation of clear-sky surface albedo [*Brooks et al.*, 1986], and parameterization of surface albedo in atmospheric process and climate models [*Briegleb and Ramanathan*, 1982; *Oleson et al.*, 2003] generally assume that the diurnal cycle of snow albedo depends only on SZA. In most radiation transfer models, the diurnal variation of surface albedo is assumed to be symmetric about solar noon and forced by the diurnal variation of SZA [*Song*, 1998]. Both regular and irregular changes in the surface state and atmosphere can negate this assumption [*Minnis et al.*, 1997; *Pirazzini*, 2004; *Pirazzini et al.*, 2006]. Consequently, sun-synchronous satellites should consider the diurnal variation of surface albedo or else risk biasing the monthly or daily mean values composed from measurements taken instantaneously once daily [*Minnis et al.*, 1997].

[8] Several studies analyze the diurnal variation of snow albedo, yet these studies are most short-term or experimental campaign measurements that focus on a single station/region [*Carroll and Fitch*, 1981; *Warren et al.*, 1998; *Winther et al.*, 2002; *Pirazzini*, 2004; *Pirazzini et al.*, 2006; *Wuttke et al.*, 2006; *Meinander et al.*, 2008]. To our knowledge, no studies have yet been conducted to examine and snow albedo's diurnal and seasonal variation in both polar regions at the same time. Satellites provide near global coverage of snow albedo, though with temporal resolution too coarse and accuracy too low to capture diurnal variations. Fortunately, the relatively long-term World Climate Research Programme (WCRP) Baseline Surface Radiation Network (BSRN) in the World Radiation Monitoring Center (WRMC) provides quality-controlled and consistent downwelling and upwelling solar irradiance measurements throughout the world, and thus offers us a chance to analyze the snow albedo's diurnal and seasonal variations in both polar regions with multiyear data sets. This study will, for the first time, systematically quantify and intercompare the multiyear mean amplitude of snow albedo's diurnal and seasonal variations at the four Arctic and Antarctic stations where high quality measurements are available to elucidate similarities and differences in snow albedo cycles across geographic zones, and to assess how diurnal changes in snow albedo affect the surface energy budget.

2. Study Sites and Data

[9] Four BSRN stations (Table 1) reside in the Arctic or Antarctica. Two stations (Barrow (BAR) and Ny-Ålesund

Table 1. Four Baseline Surface Radiation Network Stations in the Arctic and Antarctica

Station ID	Area Name	Sponsor	Surface/Topography Type	Elevation (m)	Latitude	Longitude
22 (BAR)	Barrow, Alaska, USA	United States	tundra; flat, rural.	8	71.323	−156.607
11 (NYA)	Ny-Ålesund, Spitsbergen	Germany/Norway	tundra; mountain valley	11	78.925	11.950
13 (GVN)	Georg von Neumayer, Antarctica	Germany	iceshelf; flat, rural	42	−70.650	−8.250
26 (SPO)	South Pole, Antarctica	United States	glacier, accumulation area; flat, rural	2800	−89.983	−24.799

(NYA)) are in coastal areas of Barrow, Alaska and Ny-Ålesund Island, Spitsbergen, and are seasonally snow covered over 8 months from late September to early June. The other two stations are located on the coast (Georg von Neumayer (GVN)) and at the South Pole (SPO) of Antarctica. Both are on the ice sheet and experience perennial snow. The South Pole is 2800 m above sea level while the other three coastal stations have elevation less than 50 m. Ny-Ålesund is located in a tundra mountain valley, while the other three stations are situated in flat and near uniform areas. These stations lie in areas with high surface reflectance, little grass (Barrow) or no vegetation, and high SZA, and snow at the coastal stations, being also much warmer than the South Pole, are vulnerable to the warming atmosphere and adjacent oceans. Hence the long-term in situ BSRN measurements at these stations will help to increase our understanding of snow surface properties and their changes, and hence aid the improvement of surface albedo parameterizations and satellite albedo retrieval algorithms [*McArthur*, 2005].

[10] The major measurements used in this study are air temperature, shortwave (SW) broadband total downwelling (SWD) and upwelling (SWU) radiation fluxes, and the direct (DIR) and diffuse (DIF) components of the solar insolation. The air temperature at 2 m height is measured continuously by a thermometer with uncertainty of ±0.3°C. The SW broadband solar radiation (SWD, SWU and DIF) are measured by two types of pyranometers horizontally

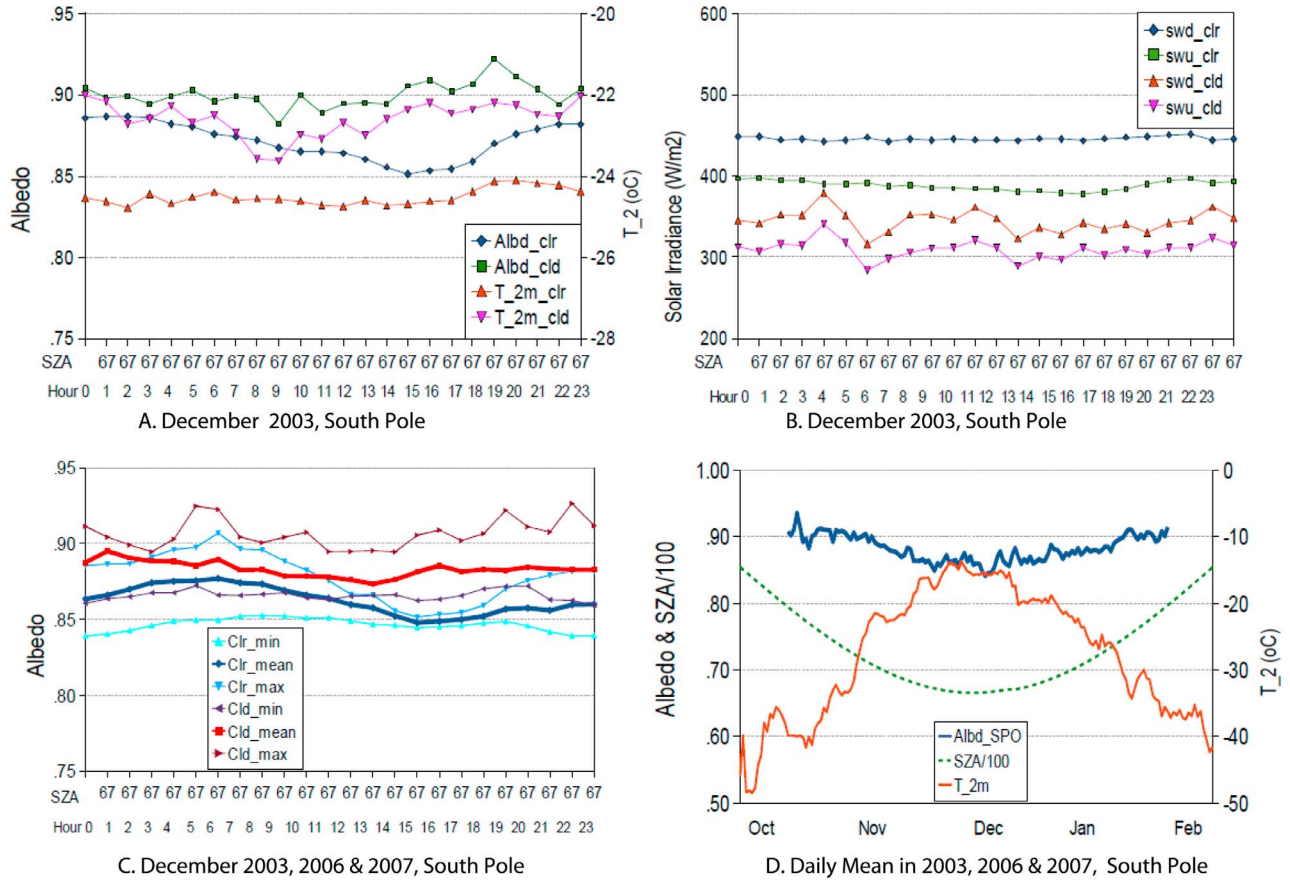

Figure 1. (a) The monthly mean diurnal cycle of snow albedo and air temperature and (b) the shortwave broadband total downwelling (SWD) and upwelling (SWU) solar irradiance for clear sky (26 days) and cloudy sky (5 days) at the South Pole (SPO) in December 2003. (c) The multiyear mean diurnal cycle in December from 2003, 2006, and 2007. (d) The seasonal (daily mean from 2003, 2006, and 2007) variation of snow albedo at SPO. The SWD and SWU data in 2004, 2005, and 2008 are not used here because of instrumental problems.

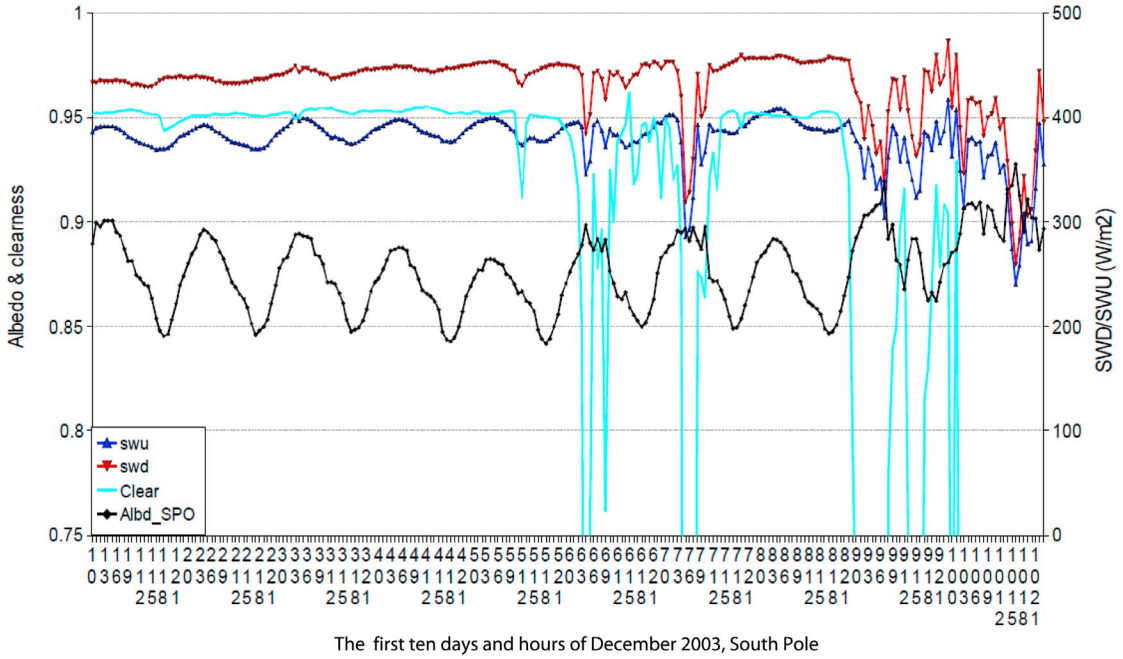

Figure 2. Diurnal cycles in the first 10 days of December 2003 at the South Pole (SPO). "Clear" is the sky clearness or cloud index (0 is overcast sky) derived from equation (1). The vertical labels for the horizontal (X) axis represent days (the first one or two numbers from day 1 to day 10) and hours (the last one or two numbers from 0, 3, …, 18, 21). The solar zenith angle in December at SPO is nearly constant at 67° with azimuth angles of 0°–360°. The maximum air temperature during these ten days was below −20°C.

positioned at a 2 m high platform within ±0.1°. Barrow and South Pole use Eppley Precision Spectral Pyranometers (PSP). Neumayer and Ny-Ålesund use Kipp and Zonen CM11 and CM21 pyranometers. DIR at the four stations is measured by Eppley Normal Incidence Pyrheliometers (NIP). The four solar radiation variables are measured separately. DIR and DIF are relative quantities, and the sum of DIR and DIF does not equal to SWD.

[11] Both Kipp and Zonen CM1/21 and Eppley PSP applied at the BSRN stations are high performance research grade pyranometers. Their spectral response ranges are 0.3–2.8 μm for CM1/21 and 0.285–2.8 μm for PSP, which cover approximately 98% of the entire solar radiation at the earth surface. Deposition of snow or frost on the dome of pyranometer is a possible error source for the BSRN measurement in both polar regions. The pyranometers (e.g., at Neumayer and Ny-Ålesund) are ventilated with slightly preheated air to minimize hoar frost problems and zero offsets during cloudless and windless conditions. The instruments are maintained continuously several times per day throughout the year when it is possible. After 1 year of operation, they are recalibrated at the German Weather Bureau according the World Radiometric Reference (WRR) [*Wuttke*, 2005]. According to the BSRN manual, the pyranometers at the South Pole and Barrow also have similar setup to remove hoar frost on the pyranometer dome [*McArthur*, 2005]. The overall measurement uncertainties are less than 2% or ±5 W/m^2 (whichever is greater) for SWD, 3% for SWU, 0.5% or ±1.5 W/m^2 for DIR, and 2% or ±5 W/m^2 for DIF when SZA is less than 75°; measurements with SZA larger than 80° are not used due to potential large errors related to the pyranometer's cosine-response quality and impacts of surface topography [*McArthur*, 2005; *Kipp and Zonen*, 2006]. Thus, this study restricts its focus to measurements with SZA less than 75°.

[12] The solar irradiances are sampled once per second and stored as 1 min averages. These 1 min mean irradiance and temperature data from 2003 to 2008 are retrieved from the WRMC-BSRN website at http://www.bsrn.awi.de/en/data/data_retrieval_via_pangaea/.

[13] What does the BSRN measure and what do the measurements represent? The 2 m height platform of BSRN pyranometers lacks the necessary footprint of a more stable and robust measurement height such as ~20 m. As *Warren et al.* [1998, p. 25,792] point out, "[f]or near-surface measurements to be applicable to interpretation of satellite measurements, it is therefore important to view a 'footprint' of surface area sufficiently large to contain a representative distribution of sastrugi slopes." This means the radiation flux measurements should be made from an elevated platform, e.g., a 22 m walk-up tower at the South Pole Station [*Warren et al.*, 1998].

[14] However, the 2 m height of BSRN radiation flux measurements is commonly employed in the snow albedo measurement community, such as in BSRN, Greenland Climate network (GC-Net) and other short-term measurements [*Seckmeyer et al.*, 2001; *Pirazzini*, 2004; *Wuttke et al.*, 2006; *Wang and Zender*, 2010b]. The viewing angle of the down-facing pyranometer is 180°, and most of the upwelling shortwave/solar radiation (SWU) received by the instrument

Table 2. Mean Number of Days at Each Hour for Clear and Cloudy Skies and the Daily Average in Each Month at Four BSRN Stations[a]

	Ny-Ålesund, April		Barrow, May		Neumayer, December		South Pole, December	
	Clear	Cloud	Clear	Cloud	Clear	Cloud	Clear	Cloud
0	8	23	5	26	12	19	25	6
1	11	21	6	25	12	19	24	7
2	11	20	8	24	11	20	26	5
3	13	18	7	24	12	19	27	4
4	14	17	7	24	12	19	27	4
5	13	18	7	24	12	19	26	5
6	15	16	8	23	13	18	27	4
7	15	17	8	23	12	19	26	5
8	15	16	10	22	14	18	27	4
9	17	14	9	22	13	18	27	4
10	16	15	10	21	13	18	27	4
11	16	15	9	22	13	18	27	4
12	16	15	10	21	14	17	28	3
13	15	16	12	20	13	18	27	4
14	16	16	10	21	12	19	26	5
15	16	15	9	22	12	19	27	4
16	14	18	8	23	13	19	26	5
17	13	18	8	23	13	18	26	5
18	12	20	9	22	13	18	26	5
19	11	20	8	23	13	18	27	4
20	11	20	9	22	13	18	28	3
21	10	21	9	22	12	19	27	4
22	9	22	8	23	12	19	26	5
23	9	23	6	25	11	20	26	5
Mean days	13	18	8	23	12	19	26	5
Daily SWD	159	86	300	231	417	308	446	370
SWD reduction[b]	73 W/m^2	46%	69 W/m^2	23%	109 W/m^2	26%	76 W/m^2	17%
Daily Albedo1	0.75	0.82	0.78	0.80	0.8	0.85	0.86	0.88
Daily Albedo2	0.78 (for all sky)	0.78 (for all sky)	0.80	0.80	0.83	0.83	0.87	0.87
Daily ASR1	39	16	65	45	83	45	61	43
Daily ASR2	26	26	51	51	60	60	59	59

[a]Mean is for the years 2003–2008; daily average measured over 24 h period. The daily albedo1 and ASR1 are for clear and cloudy sky days separately, and the daily albedo2 and ASR2 are for both clear and cloudy sky days.
[b]SWD reduction is (Clr − Cld)/Clr.

comes from the area immediately below it. If the SWU is isotropically distributed, a total of 50%, 90%, and 99% of the flux intercepted by the downfacing pyranometer comes from circular areas centered on the vertical projection of the sensor and radius respectively long 1, 3, and 10 times the height of the instrument above the surface [*Schwerdtfeger*, 1976]. "For many practical purposes (cleaning and checking of the instruments, stability of the instrument mast under strong wind conditions) the height of the downward facing pyranometer is usually 1–1.5 m above the surface" [*Pirazzini*, 2004, p. 5]. According to *Seckmeyer et al.* [2001], albedo should be measured with two radiometers with cosine-weighted field of view at about 2 to 4 m height above the ground. *Wuttke et al.* [2006] also use a pair of 2 m high pyranometers for their measurements of spectral snow albedo at Neumayer, Antarctica. About 90% of the BSRN (2 m high pyranometer) measured flux comes from a circular area of a radius 6 m centered on the vertical projection of the sensor. This area may enclose one or several snow dunes and sastrugi, not enough to sample a representative distribution of surface features instantaneously [*Warren et al.*, 1998]. However, this study focuses on climatological averages: "[w]hen the radiation instruments are near the surface in a sastrugi field, the sampling bias could be avoided by collecting a large number of samples at various places, or a long record of measurements if the sastrugi change over time [*Carroll and Fitch*, 1981]" [*Pirazzini*, 2004, p. 4]. Multiyear measurements such as in this study can capture the changing surface features of the radiometer footprint. This partially compensates for the limited pyranometer sampling area and explains why there is so much variation of the instantaneous measurements about the climatological mean.

Table 3. Statistical Results of the Surface Albedo at the Monthly and Annual Time Scales at Four Stations Examined

	Ny-Ålesund	Barrow	Neumayer	South Pole
Annual mean albedo 2003–2008	0.47	0.49	0.84	0.88
Annual mean albedo standard deviation 2003–2008	0.01	0.03	0.01	0.01
Maximum/month in monthly means 2003–2008	0.78, April	0.82, April	0.89, October	0.91, October
Minimum/month in monthly means 2003–2008	0.15, August	0.17, August	0.83, December	0.86, December
Maximum-minimum (seasonal variation amplitude)	0.63	0.65	0.06	0.05
Monthly standard deviation in a summer month within 6 years	0.01, April	0.02, May	0.01, December	0.02, December
Percentage of monthly standard deviation in the seasonal amplitude	2%	3%	17%	40%

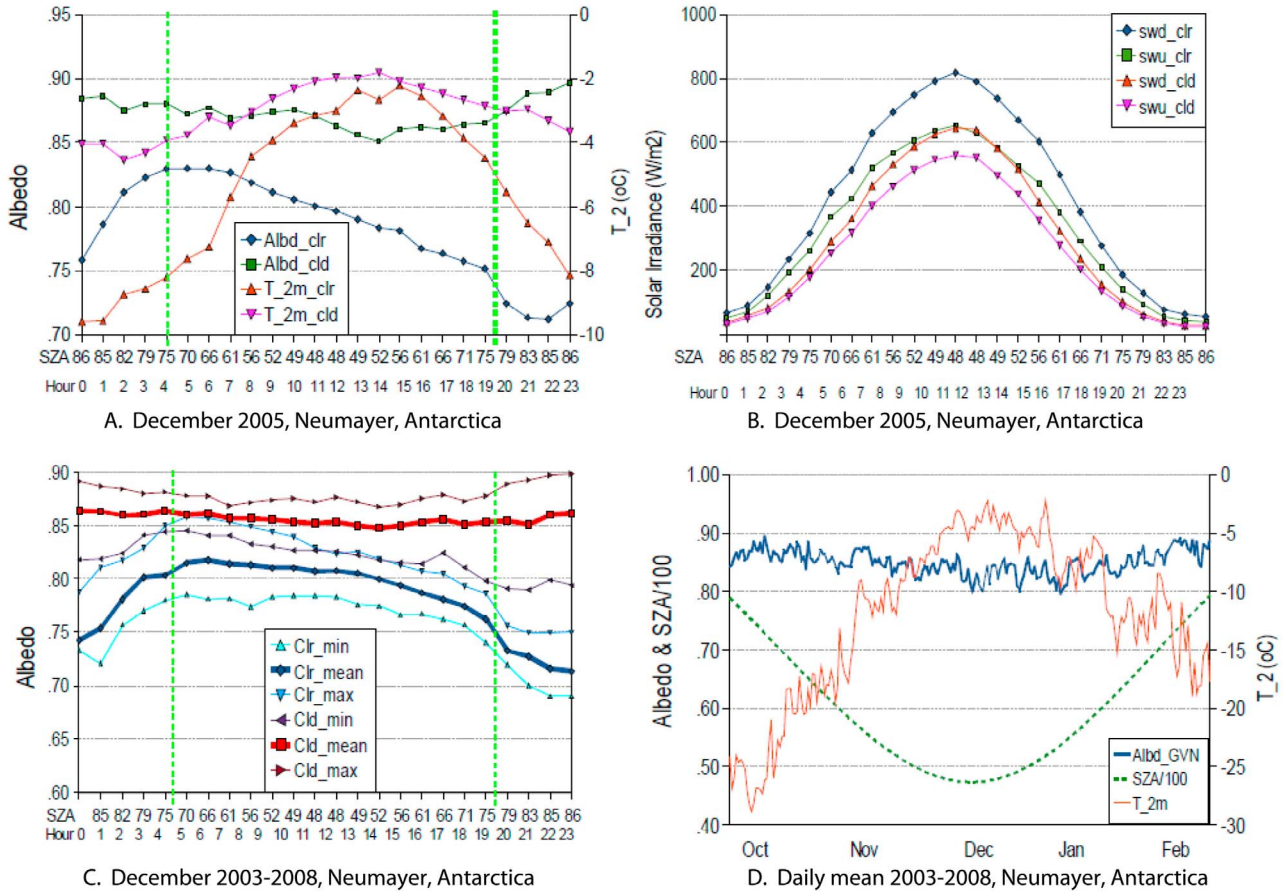

Figure 3. (a) The mean diurnal cycle of snow albedo and air temperature and (b) the shortwave broadband total downwelling and upwelling solar irradiance for clear sky (12 days) and cloudy sky (19 days) at Georg von Neumayer (GVN) in December 2003. (c) The hourly mean diurnal cycle in December from 2003 to 2008. (d) The seasonal (daily mean from 2003 to 2008) variation of snow albedo. The snow albedo values in clear sky days when the solar zenith angle (SAZ) is larger than 75° (Figure 3a) beyond two vertical lines are not reliable because of the pyranometer's cosine-response error at large SZAs.

In this study, we did not make any direct comparison with instantaneous or long-term satellite measurements. We do not know how broadly representative the 2 m height pyranometer measurements are. That would be the subject of a worthwhile study in its own right. Two qualities of the BSRN measurements deserve restatement: First, what is measured by climatological means of 2 m high radiometers may not be the albedo as measured at 20 m (or 200, or 2000 m), though, it is, because of the 6 year averaging, a well-defined climatological index of reflectance. It may contain offsets from the "true" (high tower) albedo, yet this study is concerned with the shape of the diurnal albedo curve, not with its absolute value. Second, BSRN data are the only quality controlled high precision radiometric in situ data available.

3. Data Processing

[15] One minute average irradiance data are first passed through Dixon's Q-Test to screen out random outliers in a moving window of five consecutive records at a 95% confidence level [*Miller and Miller*, 1993], and then processed into hourly means by a simple arithmetic average for values larger than 5 W/m^2, the SWD measurement uncertainty. These hourly data are further used to analyze the mean diurnal cycle within a month, which is the mean value during each hour from 0:00 to 23:00 within the 30/31 days of a month. Finally, the surface albedo is calculated using the mean SWU divided by the mean SWD at each hour. The clearness (or cloud) index in equation (1) is a simplified normalized diffuse ratio variability test of clear sky [*Long and Ackerman*, 2000].

$$clr = \frac{DIR}{DIR + DIF} \tag{1}$$

where clr is the clearness index of the sky and range from 0 (overcast) to 1 (clear). Clr is normally less than 0.95 because of atmospheric aerosols. Hours with clr < 0.3 are defined as cloudy sky. The mean clr value on cloudy days is less than 0.05, which implies that clouds, when present, are optically thick.

[16] All analysis are carried out at four time scales: (1) ten continuous diurnal cycles (hourly interval) including cloudy and clear sky days; (2) monthly mean diurnal cycles in December for the South Pole and Neumayer, in May for

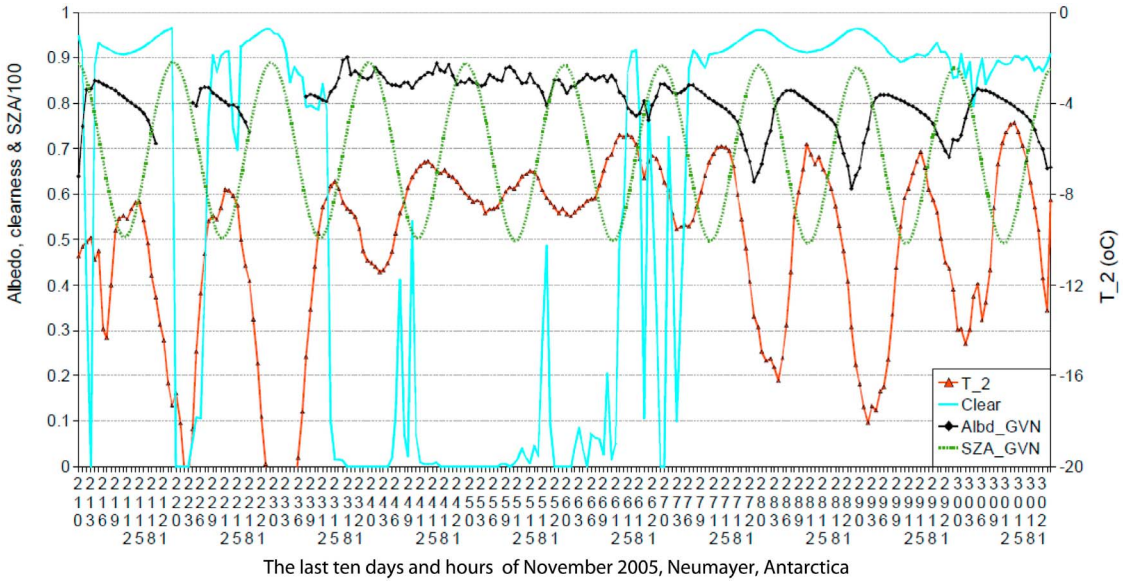

Figure 4. Diurnal cycles of in situ snow albedo, air temperature, and cloud index in the last 10 days of November 2005 at Georg von Neumayer (GVN). "Clear" is the sky clearness or cloud index (0 is overcast sky, 1 is cloudless sky) derived from equation (1). The vertical labels for the horizontal (X) axis represent days (the first two numbers from day 21 to day 30) and hours (the last one or two numbers from 0, 3, …, 18, 21). The solar zenith angle on 25 November at GVN varies from 49° at solar noon to 88° at 0:00.

Barrow, and in April for Ny-Ålesund when there is long/intense sunshine while snow still exists; (3) hourly minimum, mean and maximum based on the monthly mean diurnal variations from 2003 to 2008; and (4) the seasonal variation, which is the daily mean on each day from 2003 to 2008. The months (December, May, and April) selected for monthly mean diurnal cycles were chosen to sample the maximum forcing of snow albedo and its diurnal variation. The daily mean is the 24 h mean with SWD and SWU larger than 5 W/m^2. All average calculations are using SWD and SWU, and the mean albedo is finally derived from the mean SWD and SWU. The diurnal variation here refers to the difference between the daily maximal values minus the minimal values.

4. Results

4.1. The South Pole

[17] It is instructive to first examine data from South Pole since the SZA there is nearly constant within a 24 h period and, indeed, throughout December (Figure 1a). Hence the impact of SZA on the snow albedo diurnal cycle in December is negligible, though significant (~0.04 as SZA increases from 66° to 80°) at the seasonal scale (Figure 1d). Air temperatures at South Pole are usually below −20°C, though occasionally reaches −14°C in the 6 years from 2003 to 2008 (Figure 1d). Hence the snow is perennially dry, and the snow metamorphism proceeds slowly because of the extremely low air temperature (Figures 1a and 1b). However, the snow albedo at the South Pole on clear sky days still has a diurnal variation (of about 0.05) as shown in the first 10 days in December 2003 (Figure 2), which reduces to about 0.035 in the monthly mean diurnal cycle in December 2003 (Figure 1a), and to about 0.03 in the multiyear mean diurnal cycle in December from 2003 to 2008 (Figure 1c). During clear sky days, the minimum snow albedo (Clr_min) in the diurnal cycle is around 0.85, and the maximum snow albedo (Clr_max) has a similar diurnal pattern with but larger variation than the mean (Clr_mean) snow albedo (Figure 1c). The mean snow albedo varies between 0.85 and 0.88. The strong diurnal cycles disappear during cloudy skies. With constant SZA and solar radiation and extreme low air temperature, such strong clear sky diurnal cycles (up to 0.06 in Figure 2) must be associated with SAA and snow surface features, such as snow dunes, ripples and sastrugi [*Weller*, 1969; *Kuhn and Siogas*, 1978; *Carroll and Fitch*, 1981; *Warren et al.*, 1998]. Figure S1 in the auxiliary material shows a photo of snow sastrugi at the South Pole.[1] When the solar beam is parallel to the sastrugi long axis, the sides of sastrugi facing the sun receive more irradiance and correspondingly reflect more solar radiation back to the pyranometer than a flat surface, increasing the snow albedo by as much as 0.06 relative to when the solar beam is parallel to the sastrugi long axis and the sun is opposite the slope of the sastrugi [*Pirazzini*, 2004]. The 12 h intervals between the maximum and minimum snow albedo also match the relationship of SAA and sastrugi's orientation (Figure 2). The impact of sastrugi on the snow albedo is between the two extreme situations when SAA is between 0° and 180° and between 180° and 360° to the long axis of the sastrugi.

[18] The diffusion of incident solar radiation by clouds reduces snow albedo at large SZA (>66°), such as at the South Pole, since diffuse radiation has an effective SZA of ~55° [*Wiscombe and Warren*, 1980; *Warren*, 1982]. Clouds

[1] Auxiliary materials are available in the HTML. doi:10.1029/2010JF001864.

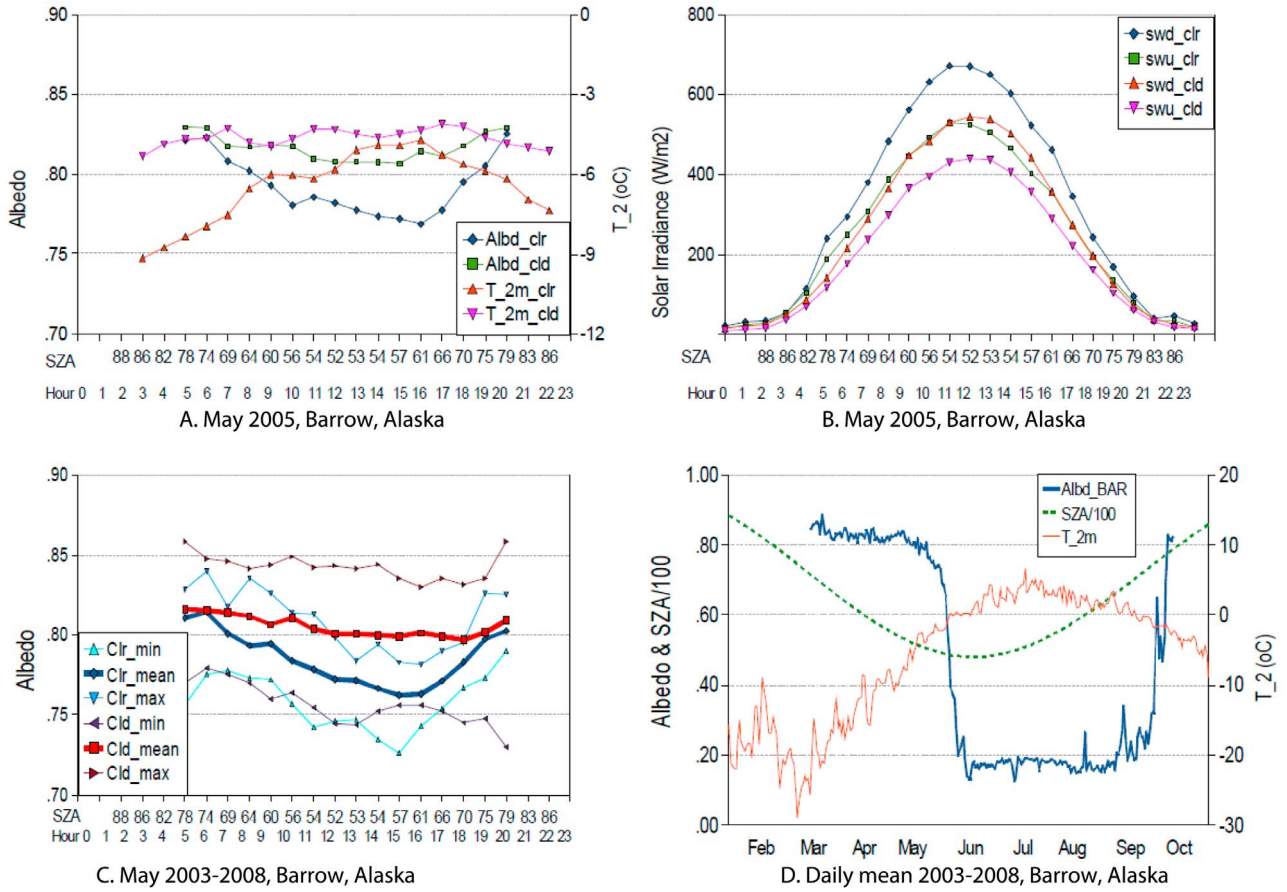

Figure 5. (a) The mean diurnal cycle of snow albedo and air temperature and (b) the shortwave broadband downwelling and upwelling solar irradiance for clear sky (8 days) and cloudy sky (23 days) at Barrow, Alaska, in May 2005. (c) The hourly mean diurnal cycle in May from 2003 to 2008. (d) The seasonal (daily mean from 2003 to 2008) variation.

also shift the spectral distribution of the incident solar radiation toward the visible due to the high absorption of water vapor and liquid water in near infrared wavelengths. The spectral shift effect exceeds the diffusion effect in most cases, and leads to a net increase in the integrated snow albedo [*Grenfell and Maykut*, 1977]. Figure 1a confirms that snow albedo on cloudy days has higher values than on clear sky days. Clouds also diminish the impact of SAA and sastrugi on snow albedo's diurnal cycle by diffusing the incident solar radiation (Figures 1a and 2). This supports the interpretation that the strong diurnal cycle of snow albedo at the South Pole is likely caused by snow sastrugi or other inhomogeneous surface features. Since the atmosphere at the South Pole is nearly transparent and only 5 days have thin cloud in December (Table 2), the diurnal cycle of snow albedo is dominated by the clear-sky patterns. At the daily scale, the mean snow albedo in December on cloudy days (0.88) is only 0.02 higher than on clear sky days (0.86), with a mean value of 0.87 in December for both clear and cloudy days. The annual mean and standard deviations of snow albedo from 2003 to 2008 is 0.88 and 0.01, with a maximum (0.91) monthly mean snow albedo in October and a minimum (0.86) in December (Table 3).

4.2. Georg von Neumayer

[19] Neumayer is on the coast of Queen Maud Land and the Weddell Sea, where cloudy days, snow fall and drifting snow are frequent [*Pirazzini*, 2004]. The snow albedo has a diurnal asymmetry with larger values in the morning and smaller values in the afternoon (Figures 3a and 3c). This diurnal asymmetry also exists in other months from October to February (Figure S2, panel A4), and is consistent with other observations near this station [*Pirazzini*, 2004; *Wuttke et al.*, 2006]. The much lower albedo value before 04:00 (solar time) and after 19:00 are likely related to the instrument measurement errors because the pyranometer has poor cosine-response quality at SZAs larger than 75° for CM1/21 [*McArthur*, 2005; *Kipp and Zonen*, 2006]. For instance, on clear sky days on 27, 28, 29, and 30 November 2005 (Figure 4), a much lower snow albedo exists when SZAs exceed 75°. The air temperature is lower than −8°C, thus snowmelting and liquid water content in snow are negligible and cannot explain the low snow albedo values at such large SZAs and low air temperature. In contrast, when clouds were present on days 23, 24, 25 and 26 in the same month, the strong diurnal cycles disappeared, and the snow albedo increased to a near

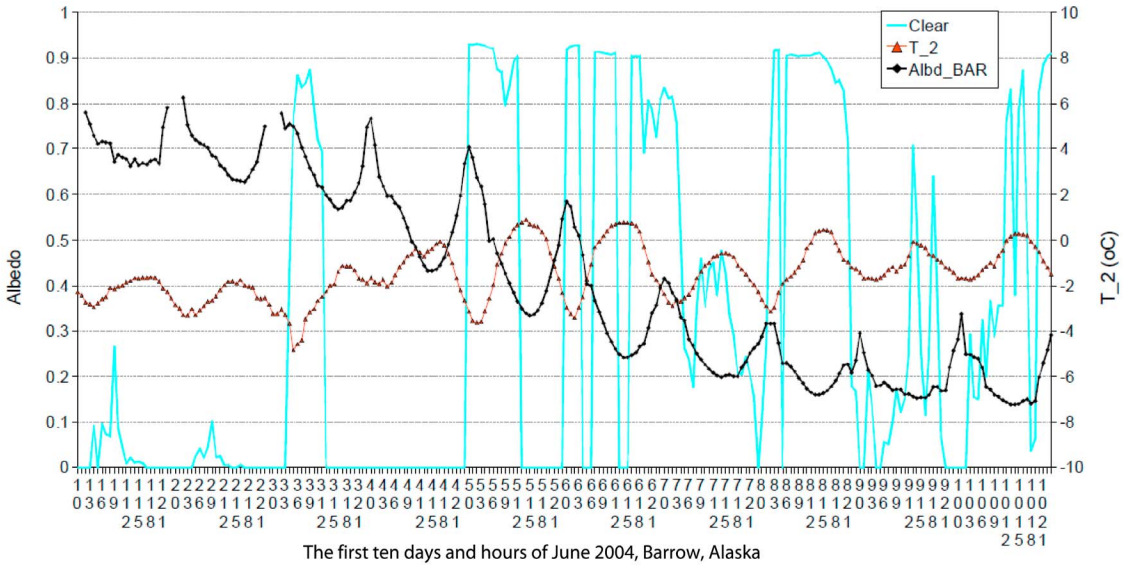

Figure 6. Diurnal cycles of in situ snow albedo, air temperature, and cloud index in the first 10 days of June 2004 at Barrow, Alaska. "Clear" is the sky clearness or cloud index (0 is overcast sky) derived from equation (1). The vertical labels for the horizontal (X) axis represent days (the first one or two numbers from day 1 to day 10) and hours (the last one or two numbers from 0, 3, …, 18, 21). The solar zenith angle on 5 June varies from 49° at local noon to 85° at local 23:00. The sun is always above the horizon during this period.

constant value of ~0.85 for SZAs larger than 75°. Moreover, the asymmetry of snow albedo still exists under the lower air temperatures (<−15°C) of October and February. This suggests that the diurnal cycles of snow albedo are likely related to snow surface features and SAA.

[20] On 15 December, SZA varies from 48° at noon to 86° at 23:00, while the snow albedo peaks at 0.83 from 04:00–06:00, then falls to 0.75 from 18:00–19:00 in a reliable SZA range of the pyranometer (Figure 3a). This is approximately a 12 h difference between the maximum and minimum reliable albedo value. This 12 h difference coincides with the sun azimuth cycle, indicating that the diurnal asymmetry is associated with surface features and SAA. This is consistent with the reported strong wind conditions (mean and maximum wind speed of 9 m/s and 35 m/s) and frequent drifting snow episodes at Neumayer [*König-Langlo and Herber*, 1996; *Pirazzini*, 2004]. The larger SZA in the morning also contributes to a higher albedo. Meanwhile, the air temperature is close to zero in the daytime and drops below −8°C in the early morning in clear skies; surface hoar crystals form at "night" and early morning, and then sublimate because of warming in the afternoon. This cycle happens every day and could partially explain the diurnal asymmetry of snow albedo variation [*McGuffie and Henderson-Sellers*, 1985; *Pirazzini*, 2004; *Domine et al.*, 2009]. In contrast, at the seasonal time scale, the near symmetric distribution of the seasonal snow albedo is likely related to the symmetric distribution of SZAs and other SZA/time-related factors (Figure 3d). A similar symmetric distribution of seasonal snow albedo also occurs in Greenland [*Wang and Zender*, 2010a, 2010b]. The annual mean and standard deviations of snow albedo from 2003 to 2008 is 0.84 and 0.01, with a maximum (0.89) monthly mean snow albedo in October and a minimum (0.83) in December (Table 3).

[21] Snow albedo at Neumayer is larger (0.06 at ~5:00 to 0.12 at ~18:00) on cloudy than clear sky days (Figures 3a, 3c, and 4). As mentioned earlier, clouds alter snow albedo by shifting the spectral distribution of surface insolation to visible wavelengths, where snow is more reflective. The magnitude of spectral shifting is related to the amount and type of cloud and column water vapor. At the South Pole, the daily SWD difference (clear-cloud) between clear and cloudy days in December is 76 W/m^2 or 17% of SWD in clear sky, leading to 0.02 higher albedo on cloudy days than on clear days (Figure 1c and Table 2). At Neumayer, the daily SWD difference in December is 109 W/m^2 or 26% of SWD in clear sky, leading to 0.05 higher albedo on cloudy days (Figure 3c and Table 2). Clouds also diffuse insolation and diminish the effects of surface features (sastrugi) and SZA on the diurnal cycle of snow albedo. The nearly constant snow albedo on cloudy days (Figures 3a, 3c, and 4) further suggests that the diurnal asymmetry on clear sky days at Neumayer is related to snow surface features.

4.3. Barrow, Alaska

[22] Snow at Barrow usually begins to melt and disappear in June, and then accumulates again beginning in late September or October (Figure 5d). The annual mean and standard deviations of snow/surface albedo from 2003 to 2008 is 0.49 and 0.03, with a maximum (0.82) monthly mean snow albedo in April and a minimum (0.17) in August when snow melts away (Table 3). The maximum forcing of snow albedo diurnal variations at Barrow occurs in May, when snow still exists and receives strong insolation. During May,

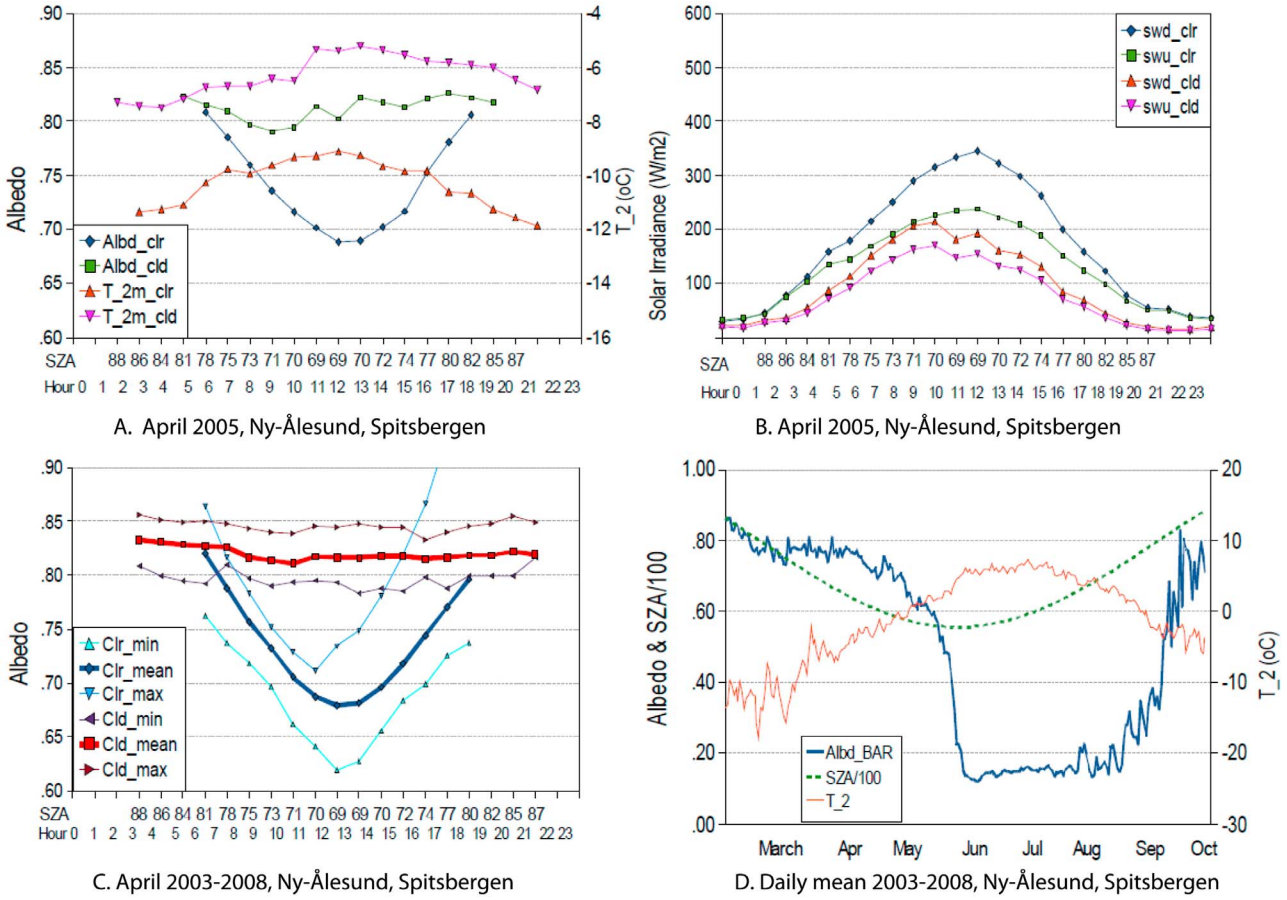

Figure 7. (a) The mean diurnal cycle of snow albedo and air temperature and (b) the shortwave broadband downwelling (SWD) and upwelling (SWU) solar irradiance for clear sky (13 days) and cloudy sky (17 days) at Ny-Ålesund, Spitsbergen, in April 2005. (c) The hourly mean diurnal cycle in April from 2003 to 2008. (d) The seasonal (daily mean from 2003 to 2008) variation and the daily values are derived from the 24 h period when both SWD and SWU are larger than 5 W/m^2.

the 23 cloudy days have smaller (−23%) SWD, higher air temperature, and also higher snow albedo than the clear sky days (Figures 5a–5c and Table 2). In contrast, the snow albedo has strong diurnal cycles on clear sky days, and only weak diurnal cycles on cloudy days, when clouds diffuse insolation and thus diminish the impact of SZA and snow surface features on snow albedo. The asymmetry of the diurnal cycle of snow albedo, which peaks near 06:00 and reaches minimum near 15:00, coincident with maximum air temperature (near melting point), is consistent with surface hoar daily cycles that form in the late evening and morning and then sublimate in the afternoon. In contrast, in months with much lower air temperature such as in March, the diurnal cycles of snow albedo are nearly symmetric around the solar noon (Figure S2, panel A2).

[23] During the first 10 days in June 2004 (Figure 6), air temperature varies from −4°C to 1°C and the sun continuously hangs above the horizon. The melt-freeze (or wet) snow metamorphism dominates the snow albedo diurnal variation, which shows asymmetric diurnal cycles, maximal in the morning and minimal in the late afternoon (15:00–18:00). Snow albedo recovers after 18:00, presumably due to refreezing when the air temperature drops below the freezing point. When snow completely melts away on days 8, 9 and 10, the surface albedo has a symmetric diurnal cycle with a minimum value around noon, consistent with soil albedo dependence on SZA [*Wang et al.*, 2005].

4.4. Ny-Ålesund, Spitsbergen

[24] The annual mean and standard deviations of snow/surface albedo at Ny-Ålesund from 2003 to 2008 is 0.47 and 0.01, with a maximum (0.78) monthly mean snow albedo in April and a minimum (0.15) in August when snow melts away (Table 3). Snow at Ny-Ålesund disappears as early as in May (Figure 7d) some years, earlier than at Barrow, hence April is the month of maximum snow forcing. The mean diurnal cycle of snow albedo in April (Figures 7a–7c) has a near symmetric diurnal cycle on clear sky days, minimal at noon and maximal in both morning and afternoon. In April 2005 (Figure 7a), the clear sky snow albedo increases from 0.69 at noon to 0.81 in the morning and afternoon when SZA is ~80°. The low air temperature (<−5°C) and small solar radiation variation (<350 W/m^2)

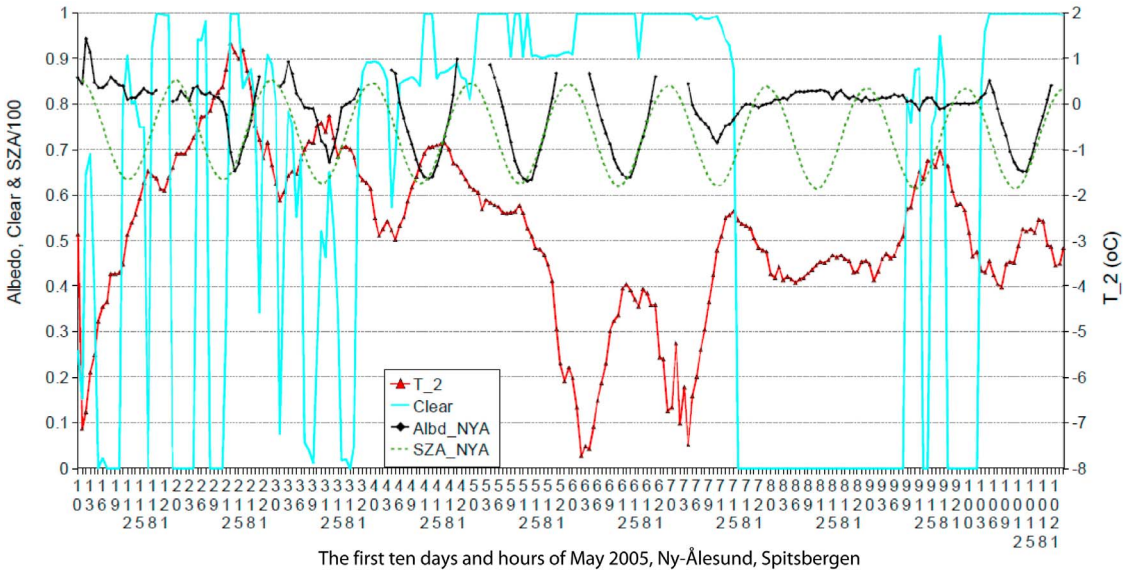

Figure 8. Diurnal cycles of in situ snow albedo, air temperature, and cloud index in the first ten days of May, 2005, at Ny-Ålesund (NYA), Spitsbergen. "Clear" is the sky clearness or cloud index (0 is overcast sky) derived from equation (1). The vertical labels for the horizontal (X) axis represent days (the first one or two numbers from day 1 to day 10) and hours (the last one or two numbers from 0, 3, …, 18, 21). The Solar Zenith Angle (SZA) on May 5 varies from 62° at local noon to 85° at local 23:00. The sun is always above the horizon during this period.

indicate that the impact of snow metamorphism and surface hoar cycles on the diurnal cycle at Ny-Ålesund is small, and perhaps negligible since both effects would lead to the asymmetric diurnal variation of snow albedo as shown in Barrow and Neumayer. Snow albedo is nearly constant and up to 0.12 higher on cloudy than clear days, which are ~4°C colder (Figure 7a). Other factors in addition to SZA, such as snow surface features (snow dunes, sastrugi, etc.) and/or shadowing, are required to explain the large clear sky diurnal variations.

[25] The first ten diurnal cycles in May 2005 at Ny-Ålesund (Figure 8) include both clear and cloudy days. On clear sky days 4, 5, 6 and 10, snow albedo shows symmetric diurnal cycles minimal at solar noon. This is the only site of the four we examined where the diurnal cycle of snow albedo matches most radiation transfer model assumptions: the diurnal variation of surface albedo is symmetric and forced by the diurnal variation of SZA [*Song*, 1998; *Oleson et al.*, 2003]. However, the diurnal cycle is much larger than what models typically predict [*Song*, 1998; *Wang and Zender*, 2010a]. The large diurnal variation (up to 0.2) of snow albedo suggests that snow surface features somehow amplify SZA effects to create the large and symmetric diurnal cycles. In fact, there are strong easterly winds (mean and maximum wind speed: 6 and 27 m/s) and wind-channeled easterly oriented sastrugi at Ny-Ålesund [*König-Langlo and Herber*, 2006]. The long axis of easterly oriented sastrugi is parallel to the sun beam in the early morning and in the late afternoon, leading to higher snow albedo in the morning and in the afternoon and smaller snow albedo at noon when the sun beam is vertical to the long axis of the sastrugi, thus magnifying the snow albedo diurnal variations [*König-Langlo and Herber*, 2006; *Pirazzini*, 2004]. On cloudy days 8 and 9, the snow albedo is larger and nearly constant. Clouds exist over half of April, reduce SWD by 46%, and increase snow albedo by 0.07 at the daily scale (Table 2).

4.5. ASR Difference

[26] The diurnal variations observed at the four BSRN stations show that instantaneous observations of snow albedo at certain times of a day (e.g., sun-synchronous satellite measurements) will, if naively extrapolated to daily or longer timescale averages, lead to systematic biases in the surface energy budget. To quantify the potential biases incurred by extrapolating instantaneous albedos to 24 h mean albedos, we compare the difference between the absorbed solar radiation (ASR_0) from the 24 h mean SWD and SWU, and the ASR derived from the 24 h mean SWD and the instantaneous albedo within each hour (Figure 9), which is assumed to represent the satellite-derived daily (or 24 h mean) albedo. Thus, the ASR difference (ASR-ASR_0) is assumed to represent the 24 h (or daily) mean difference between satellite measurements and in situ measurements, and the patterns (ASR-ASR_0) are opposite to the diurnal cycles of snow albedo (Figures 1a, 3a, 5a, and 7a). Daily ASR differences vary from −20 to 12 W/m^2 at Ny-Ålesund, from −16 to 9 W/m^2 at Barrow, from −7 to 20 W/m^2 at Neumayer, and from −6 to 6 W/m^2 at the South Pole. Taking the equatorial overpass times of satellites Terra (10:30) and Aqua (13:30) as examples, the ASR difference at 10:30 is close to zero for Barrow, and −3, −1, and 10 W/m^2 for the South Pole, Neumayer, and Ny-Ålesund, respectively; the ASR difference at 13:30 is near zero at Neumayer and 4, 5, and 6 W/m^2 at the South Pole, Ny-Ålesund and Barrow, respectively. The 24 h mean ASR at Ny-Ålesund in April, Barrow in May, at Neumayer and the South Pole in

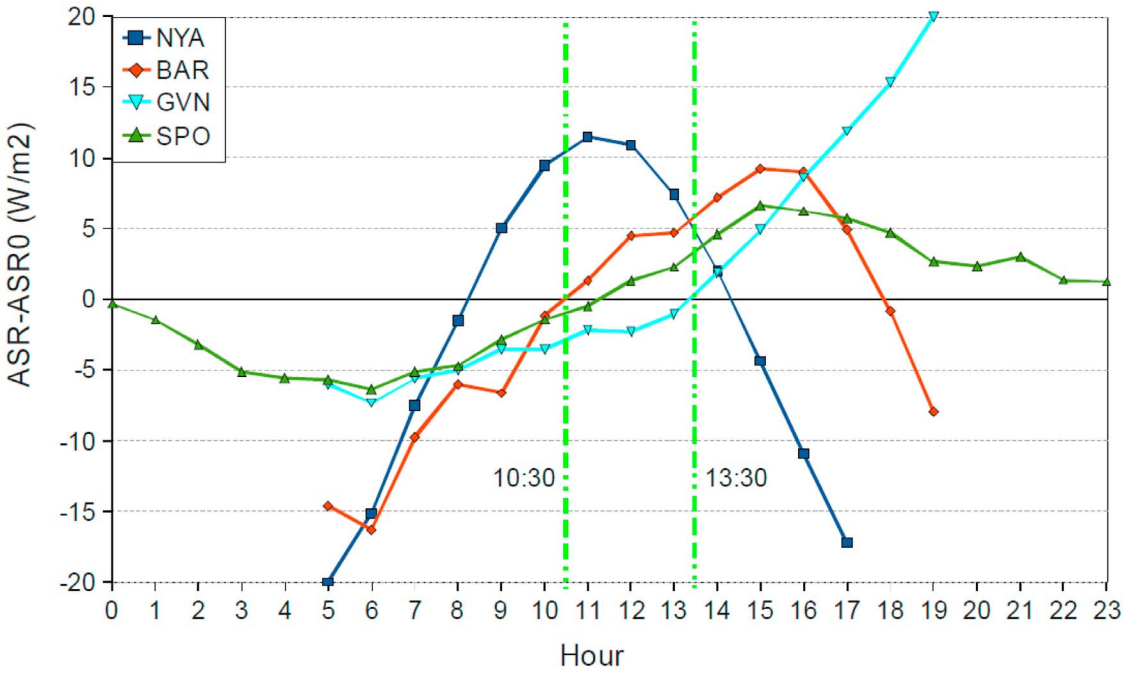

Figure 9. The daily difference of absorbed solar radiation (ASR) in clear-sky days on the snow surface derived from the daily mean SWD and SWU (ASR0) and from the daily mean SWD and one instantaneous albedo within each hour, which is assumed to represent the instantaneous albedo measurement from a sun-synchronous satellite. This instantaneous albedo also represents the daily albedo to assess the daily ASR difference for the satellite's instantaneous measurements (ASR) versus the 24 h mean value (ASR0). The daily mean ASRs at Ny-Ålesund (NYA) in April, Barrow (BAR) in May, and Neumayer (GVN) and the South Pole (SPO) in December are 39, 65, 83, and 61 W/m^2 for clear sky and 26, 51, 60, and 59 W/m^2 for the entire month for clear and cloudy sky, respectively (Table 2). The two vertical green lines indicate the equatorial pass time of the Terra and Aqua satellites that have MODIS instruments on board.

December is 39, 65, 83 and 61 W/m^2 for clear sky, and 26, 51, 60 and 59 W/m^2 for the entire month including clear and cloudy sky, respectively (Table 2).

[27] Even under ideal conditions that satellite sensors could correctly measure snow albedo, the satellite-measured snow albedo on clear days is systematically lower than the snow albedo on cloudy days (Figures 1a, 1b, 3a, 3b, 5a, 5b, 7a, and 7b). Since satellites cannot measure snow albedo under clouds, albedo parameterizations based on satellite measurements may generate systematic errors in the surface energy budget if the satellite-measured clear-sky snow albedo is used to represent the cloudy-sky snow albedo. The magnitude of errors is dependent on the amount of cloud and the downwelling solar radiation. For instance, the integrated 24 h mean ASR difference between clear sky and all sky (ASR1 – ASR2) is 13 (50%), 14 (28%), 23 (38%) and 2 (2%) W/m^2 (Table 2) at Ny-Ålesund in April, Barrow in May, at Neumayer and the South Pole in December, respectively. ASR1 is derived from the clear-sky SWD and SWU. ASR2 is derived from the monthly mean SWD and SWU for both clear and cloudy sky. Recall that these are the months of maximum forcing by snow albedo at each station. The monthly and annual mean diurnal cycles and ASR difference in each month for each station are shown in the auxiliary material (Figures S2–S5). The ASR differences generally increase from winter to summer and decline from summer to winter. The magnitude of the annual ASR difference is about one third maximum monthly ASR differences.

5. Summary and Discussion

[28] The BSRN has made available to the community precise, consistent and interannual measurements of solar radiation around the world. We use these to investigate the diurnal and seasonal variations of snow albedo, and to elucidate the difference and similarities at four BSRN stations in the Arctic and Antarctica from 2003 to 2008. The two Arctic stations (Ny-Ålesund and Barrow) experience seasonal snow cover, while the two Antarctic stations (Neumayer and the South Pole) are on the ice sheet and experience perennial snow cover. We examine the monthly mean diurnal cycle of, during periods of maximum snow albedo forcing, the early summer months of April at Ny-Ålesund and May at Barrow, and the austral summer month of December at both Neumayer and the South Pole. Each station shows unique diurnal cycles due to regionally different factors that affect snow albedo, including cloudiness, SZA, SAA, surface features, snow metamorphism, surface hoar formations and melt-freeze cycles.

[29] Clouds are a major factor in controlling the diurnal cycle of snow albedo at the four stations. Within a month, cloud cover varies from 5 days in December at the South

Pole, to 23 days in May at Barrow. Clouds reduce the daily SWD from 17% at the South Pole to 46% at Ny-Ålesund (Table 2). Clouds also have a diurnal cycle with more clear-sky days from hours 8:00 to 14:00 than in other periods at these stations. The diurnal cycle of cloud cover is most pronounced at Ny-Ålesund, where there are 16 clear-sky days from hours 9:00 to 15:00, with up to 8 clear-sky days more than at other hours (Table 2). Clouds alter the snow albedo through several ways. Clouds shift the solar radiation spectral distribution of surface insolation by backscattering to space more VIS than NIR radiation, which tends to reduce snow albedo, while simultaneously absorbing more NIR than VIS radiation which acts to increase snow albedo. In addition, multiple scattering of radiation between cloud and snow surface, aka the "snow/ice blink" effect, shifts solar insolation toward VIS wavelengths, thus increasing the snow albedo [*Grenfell and Perovich*, 2008]. The net effect of cloud absorption, backscatter and multiple scattering with the surface is to shift the surface insolation toward VIS wavelengths and increase snow albedo [*Gardner and Sharp*, 2010]. This net effect appears at all stations we examined, increasing snow albedo by 0.07, 0.02, 0.05 and 0.02 at Ny-Ålesund, Barrow, Neumayer and the South Pole respectively on cloudy days relative to clear (Table 2). Meanwhile, clouds diffuse direct solar insolation, reducing or eliminating the impact of snow surface features, SZA and SAA on snow albedo, thus changing the diurnal cycle of snow albedo [*Pirazzini*, 2004]. Indeed, the snow albedo remains nearly constant on cloudy days (Figures 1a, 4a, 7a, and 8a) at the four BSRN stations, also consistent with spectral measurements in January 2004 at Neumayer by *Wuttke et al.* [2006].

[30] Snow metamorphism is generally classified into equilibrium (or dry) metamorphism rounds, kinetic metamorphism facets, and melt-freeze (or wet) metamorphism [*Colbeck*, 1982]. Driving forces behind snow metamorphism are macroscopic snow temperature gradients and microscopic vapor pressure gradients [e.g., *Flanner and Zender*, 2006]. Dry metamorphism is normally classified into Equi-Temperature (ET) and Temperature Gradient (TG) metamorphism [*Sommerfeld and LaChapelle*, 1970]. ET takes place under gradients <10°C/m and TG for gradients >20°C/m, with a transition zone in between. Snow metamorphism converts snow grains from small to large crystals, reducing the specific surface area and thus snow albedo [e.g., *Domine et al.*, 2006; *Picard et al.*, 2009]. Metamorphism proceeds exponentially faster in warm (e.g., >−5°C) than cold snow (e.g., <−10°C), and comes to a virtual standstill at −40°C [*Colbeck*, 1983; *Taillandier et al.*, 2007]. Consistent with this behavior, the diurnal cycle and the snow albedo at the South Pole remain nearly constant on cloudy days (Figure 1a) which are all at extremely low air temperature (e.g., <−20°C). During the onset of snowmelt, e.g., in the first 6 days of June 2004 at Barrow (Figure 6), melt-freeze (wet) snow metamorphism clearly exceeds the impact of cloud on snow albedo and dominates the snow albedo diurnal cycles.

[31] Considering the irreversible processes of snow grain size increase in snow metamorphism [*Colbeck*, 1982], grain size-related snow metamorphism alone cannot explain the asymmetric or symmetric snow albedo diurnal cycles at Neumayer and Ny-Ålesund. Snow surface hoar crystals that may form at "night" and early morning, could brighten the surface from the previous day's low value, and then sublimate and darken the surface during the following afternoon warming [*Pirazzini*, 2004; *Domine et al.*, 2009]. Surface hoar may help explain the asymmetric diurnal variations of snow albedo at stations Neumayer and Barrow, assuming wind ventilation does not prevent the formation of surface hoar. Meanwhile, the asymmetric diurnal variation of snow albedo exists from austral summer to winter months at Neumayer and has larger amplitude in the winter months (Figure S2). However, surface hoar cycles cannot explain the symmetric snow albedo diurnal variation at Ny-Ålesund. Wind can accelerate grain size increase [*Cabanes et al.*, 2003] in the case of fresh snow, and wind can also fragment and partially sublimate aged crystals, reducing grain size [*Domine et al.*, 2009]. However, wind effects on crystal size distributions are unlikely to explain the snow albedo diurnal variations at Neumayer and Ny-Ålesund because the winds are much more variable than the albedo diurnal variation. Long-term wind-driven snow surface features, e.g., snow dunes and sastrugi, illuminated by the diurnal cycle of sunlight, are likely to be the primary cause of snow albedo diurnal variations at the two stations, particularly at Ny-Ålesund where the long axis of easterly oriented sastrugi caused by the strong easterly wind is parallel to the sun beam in the early morning and in the late afternoon, leading to higher snow albedo in the morning and in the afternoon and smaller snow albedo at noon when the sun beam is vertical to the long axis of the sastrugi, thus magnify the snow albedo diurnal variations [*König-Langlo and Herber*, 2006; *Pirazzini*, 2004].

[32] At Neumayer, "the occurrence of cyclones and easterly winds produced frequent snowfall and almost continuous drifting snow" [*Pirazzini*, 2004, p. 13]. According to the report of *Kupfer et al.* [2006] and *König-Langlo and Herber* [1996], Neumayer in Antarctic has higher wind speed than Ny-Ålesund, with prevailing mean and maximum wind speed of 9 m/s and 35 m/s at Neumayer, and 6 m/s and 27 m/s at Ny-Ålesund. Snow drifts could happen when wind speed exceeds 6 m/s, and snow dunes may form when wind speed exceeds 9 m/s [*Birnbaum et al.*, 2010]. Based on wind speeds, snow dunes or sastrugi may form at the two stations. Field pictures at Neumayer and Ny-Ålesund show snow dunes or snow sastrugi with different sizes exist at the two stations, and "[t]he surface is always covered with snow which forms occasionally sastrugies up to 1 m height" [*König-Langlo and Herber*, 2006, p. 1]. "The normal condition of snow in the polar regions is in the form of fields of sastrugi. Relative to a flat surface, sastrugi usually cause only a slight reduction in albedo but can alter the bidirectional reflectance pattern significantly, particularly at large view angles and especially in the forward-scattering direction" [*Warren et al.*, 1998, p. 17]. However, at all stations the impact of sastrugi, SAA and SZA can be overwhelmed by the diffusing effects of overcast cloud.

[33] SZA increases snow albedo because the increased light path over which obliquely incident photons interact with snow grains allows more multiple scattering and less penetration of and absorption by the snow surface [*Wiscombe and Warren*, 1980; *Lucht et al.*, 2000; *Flanner and Zender*, 2006]. The dependence of snow albedo on SZA is most distinct in

April and May at Neumayer (Figures 7 and 8), where snow albedo has the same diurnal symmetry as SZA. At the seasonal scale, the snow albedo at Neumayer and the South Pole has a symmetric dependence on SZA, minimal in summer and higher in spring and fall (Figures 1d and 3d). Such near-symmetric seasonal snow albedo around summer is caused together by SZA and other SZA/time-related factors (e.g., air temperature, snow aging, etc.), and also occurs in Greenland [*Wang and Zender*, 2010a, 2010b]. At Ny-Ålesund and Barrow, the seasonal snow albedo shows an increase trend with SZA, too (Figures 5d and 7d). However, at very large SZA (e.g., >80°) the shadowing effect of an uneven snow surface can decrease the snow albedo [*Warren et al.*, 1998; *Pirazzini*, 2004]. For example, on days 27–30 November 2005 at Neumayer (Figure 4), the much lower snow albedo (<0.7) when SZA > 80° is consistent with a shadowing effect by an uneven snow surface in addition to the pyranometer's cosine-response error, and to the reduction of the effective SZA by long-path atmospheric (Rayleigh and aerosol) scattering.

[34] At very large SZA (e.g., >80°), the clear sky diffusion insolation increases due to atmospheric (Rayleigh and aerosol) scattering, thus the effective SZA becomes less than the real SZA, resulting in lower snow albedo [*Wiscombe and Warren*, 1980]. At Neumayer (Figures 3 and 4), the much lower snow albedo in clear sky at SZA > 80° is consistent with reduction in effective SZA by long-path scattering, in addition to the instruments' cosine-response error and the shadowing effects of uneven snow surfaces [*Strahler et al.*, 1999; *McArthur*, 2005; *Kipp and Zonen*, 2006].

[35] In addition, other factors can affect the daily albedo cycles, such as surface tilting, hoar frost and the presence of three-dimensional features near the measurement stations. The pair of upfacing and downfacing BSRN pyranometers are horizontally positioned within ±0.1° [*McArthur*, 2005]. The effect of surface slope and the pyranometer tilting on the snow albedo diurnal cycle at Neumayer is very limited if it is not negligible since our observed diurnal trend (Figures 3 and 4) is similar with literature report [*Pirazzini*, 2004, Figure 7; *Wuttke et al.*, 2006, Figure 7]. According to *Warren et al.* [1998], the effect of surface tilting at the South Pole is negligible because the large-scale surface slope is only 0.001. The three-dimensional features only exist at Ny-Ålesund that "[i]n the south of the village the 554 m high Zeppelin mountain shades the place for several weeks in spring and fall" [*Kupfer et al.*, 2006, p. 72] and "a fan is mounted in the instrument to avoid the deposition of hoarfrost and dew as well as the heating of the dome" [*Kupfer et al.*, 2006, p. 8]. At Neumayer, "[t]he pyranometers are ventilated with slightly preheated air to minimize hoar frost problems and zero offsets during cloudless and windless conditions" [*Wuttke*, 2005, p. 4]. According to the BSRN manual, the pyranometers at the South Pole and Barrow also have similar setup to remove hoar frost on the pyranometer dome [*McArthur*, 2005]. Other factors that affect snow albedo, such as snow aging and snow impurities have little effect on the diurnal variation of snow albedo. Moreover, we also used a Dixon's Q-Test to screen out the random outlier of the averaged 1 min flux records within five consecutive minutes at the 95% confidence level [*Miller and Miller*, 1993].

[36] Last, are the 6 year data sufficient to derive a climatic mean, given the interannual variability of the meteorological conditions? According to the "long-term" (>35 years) ground records at station SANAE (World Meteorological Organization Station number: 89001; 70.10S, 357.36E), to the east of station Neumayer, air temperature at SANAE has a 4–6 years recurrent variations (not shown). A 5 year moving window is also commonly used in analyzing time series climatic data sets [*Hansen et al.*, 2006; *Arndt et al.*, 2010]. The radiation flux data records at four stations in our study are of different durations. For the cleanest intercomparison, we chose the common data record duration of 6 years. Even so, there were three 1 year gaps at the South Pole station. The 6 year record reflects typical snow albedo variations at these stations during these 6 years. The 6 year standard deviation of monthly mean albedo in summer at these stations is typically less than 0.02, whereas the seasonal cycle of monthly mean albedo is of amplitude 0.06 at two perennial snow covered stations Neumayer and the South Pole in Antarctica and 0.65 at two seasonal snow covered stations Barrow and Ny-Alesund in the Arctic (Table 3). Since the interannual standard deviation is usually 2–40% of the seasonal variation amplitude, we think this 6 year period merits the name "climatological" or conservatively a "multiyear" mean.

6. Conclusions

[37] The snow albedo at the four BSRN stations in both the Arctic and Antarctica displays different magnitudes and patterns of diurnal variation. These diurnal variations are dominated by different factors at each station, and depend on dynamically changing snow properties and environmental conditions. Satellite measured clear sky snow albedos will be lower (and thus, if treated naively, underestimate) the all-sky snow albedo. One-time instantaneous observations also lead to systematic biases if snow albedo diurnal variations are neglected. Snow albedo is, at these BSRN stations, usually not symmetric around solar noon, though the solar noon albedo is most important because of the peak solar radiation. Sometimes, e.g., for the asymmetric snow albedo diurnal variation at the South Pole and Neumayer, snow albedo near solar noon does best represent the 24 h mean snow albedo. In other locations like Ny-Ålesund, solar noon coincides with minimal snow albedo, consistent with most current climate model parameterizations, but has much larger variations than the predictions of snow and climate models. The local times most representative of 24 h mean snow albedo are 10:30, 11:30, 13:30 and 14:30 for Barrow, the South Pole, Neumayer and Ny-Ålesund, respectively. The instantaneous forcing due to the difference between instantaneous albedo and the 24 h mean albedo is up to 50% of the absorbed solar radiation. Snow-atmosphere radiative transfer models and other snow models coupled to general circulation models should also consider the diurnal variation of snow albedo in order to better represent the consequent fast time scale feedbacks, e.g., snowmelt-albedo feedback.

[38] **Acknowledgments.** We thank all the researchers who deploy, operate, and maintain the World Climate Research Programme (WCRP) Baseline Surface Radiation Network (BSRN) stations that provide the in situ measurements on air temperature, shortwave upwelling, downwelling,

and direct and diffuse solar radiation used here. We thank Florent Domine and two anonymous reviewers for their helpful and insightful comments. Funding for this work is provided by NASA NNX07AR23G; National Basic Research Program of China (973 Program) (grant 2011CB707103); Sun Yat-sen University's "Hundred Talents" program; NASA International Polar Year (IPY) Program, NASA NNX07AR23G; and NSF OPP ARC-0714088.

References

Arndt, D. S., M. O. Baringer, and M. R. Johnson (2010), State of the climate in 2009, *Bull. Am. Meteorol. Soc.*, *91*, s1–s222, doi:10.1175/BAMS-91-7-StateoftheClimate.

Birnbaum, G., et al. (2010), Strong-wind events and their influence on the formation of snow dunes: Observations from Kohnen station, Dronning Maud Land, Antarctica, *J. Glaciol.*, *56*, 891–902, doi:10.3189/002214310794457272.

Briegleb, B. P., and V. Ramanathan (1982), Spectral and diurnal variations in clear sky planetary albedo, *J. Clim. Appl. Meteorol.*, *21*, 1160–1171, doi:10.1175/1520-0450(1982)021<1160:SADVIC>2.0.CO;2.

Brooks, D. R., E. F. Harrison, P. Minnis, J. T. Suttles, and R. S. Kandel (1986), Development of algorithms for understanding the temporal variability of the Earth's radiation balance, *Rev. Geophys.*, *24*, 422–438, doi:10.1029/RG024i002p00422.

Cabanes, A., L. Legagneux, and F. Domine (2003), Rate of evolution of the specific surface area of surface snow layers, *Environ. Sci. Technol.*, *37*, 661–666, doi:10.1021/es025880r.

Carroll, J. J., and B. W. Fitch (1981), Effects of solar elevation and cloudiness on snow albedo at the South Pole, *J. Geophys. Res.*, *86*, 5271–5276, doi:10.1029/JC086iC06p05271.

Colbeck, S. C. (1982), An overview of seasonal snow metamorphism, *Rev. Geophys.*, *20*, 45–61, doi:10.1029/RG020i001p00045.

Colbeck, S. C. (1983), Theory of metamorphism of dry snow, *J. Geophys. Res.*, *88*, 5475–5482, doi:10.1029/JC088iC09p05475.

Domine, F., R. Salvatori, L. Legagneux, R. Salzano, M. Fily, and R. Casacchia (2006), Correlation between the specific surface area and the short wave infrared (SWIR) reflectance of snow, *Cold Reg. Sci. Technol.*, *46*, 60–68, doi:10.1016/j.coldregions.2006.06.002.

Domine, F., A. S. Taillandier, A. Cabanes, T. A. Dougla, and M. Sturm (2009), Three examples where the specific surface area of snow increased over time, *Cryosphere*, *3*, 31–39, doi:10.5194/tc-3-31-2009.

Flanner, M. G., and C. S. Zender (2006), Linking snowpack microphysics and albedo evolution, *J. Geophys. Res.*, *111*, D12208, doi:10.1029/2005JD006834.

Flanner, M. G., C. S. Zender, J. T. Randerson, and P. J. Rasch (2007), Present-day climate forcing and response from black carbon in snow, *J. Geophys. Res.*, *112*, D11202, doi:10.1029/2006JD008003.

Gardner, A. S., and M. J. Sharp (2010), A review of snow and ice albedo and the development of a new physically based broadband albedo parameterization, *J. Geophys. Res.*, *115*, F01009, doi:10.1029/2009JF001444.

Grenfell, T. C., and G. A. Maykut (1977), The optical properties of ice and snow in the Arctic Basin, *J. Glaciol.*, *18*, 445–463.

Grenfell, T. C., and D. K. Perovich (2008), Incident spectral irradiance in the Arctic Basin during the summer and fall, *J. Geophys. Res.*, *113*, D12117, doi:10.1029/2007JD009418.

Hall, A. (2004), The role of surface albedo feedback in climate, *J. Clim.*, *17*, 1550–1568, doi:10.1175/1520-0442(2004)017<1550:TROSAF>2.0.CO;2.

Hansen, J., M. Sato, R. Ruedy, K. Lo, D.W. Lea, and M. Medina-Elizade (2006), Global temperature change, *Proc. Natl. Acad. Sci. U. S. A.*, *103*, 14,288–14,293, doi:10.1073/pnas.0606291103.

Jin, Y., C. B. Schaaf, C. E. Woodcock, F. Gao, X. Li, A. H. Strahler, W. Lucht, and S. Liang (2003), Consistency of MODIS surface bidirectional reflectance distribution function and albedo retrievals: 2. Validation, *J. Geophys. Res.*, *108*(D5), 4159, doi:10.1029/2002JD002804.

Kipp and Zonen (2006), CMP series pyranometer instruction manual, version 0806, user guide, Delft, Netherlands. [Available at http://www.kippzonen.com/.]

König-Langlo, G., and A. Herber (1996), The meteorological data of the Neumayer station (Antarctica) for 1992, 1993, and 1994, *Rep. Polar Res. 187*, Alfred Wegener Inst. for Polar and Mar. Res., Bremerhaven, Germany.

König-Langlo, G., and A. Herber (2006), Bipolar Intercomparison of long-term solar radiation measurements from two BSRN stations, paper presented at the 9th Science and Review Workshop for the BSRN, Lindenberg, Germany, 29 May–02 Jun.

Kuhn, M., and L. Siogas (1978), Spectroscopic studies at McMurdo, South Pole and Siple stations during the austral summer 1977–78, Antarct, *J. U. S.*, *13*, 178–179.

Kupfer, H., A. Herber, and G. König-Langlo (2006), *Radiation Measurements and Synoptic Observations at Ny-Ålesund, Svalbard*, *Ber. Polarforsch. Meeresforsch.*, 538, 104 pp.

Long, C. N., and T. P. Ackerman (2000), Identification of clear skies from broadband pyranometer measurements and calculation of downwelling shortwave clouds effects, *J. Geophys. Res.*, *105*, 15,609–15,626, doi:10.1029/2000JD900077.

Lucht, W., C. B. Schaaf, and A. H. Strahler (2000), An algorithm for the retrieval of albedo from space using semiempirical BRDF models, *IEEE Trans. Geosci. Remote Sens.*, *38*, 977–998, doi:10.1109/36.841980.

McArthur, L. J. B. (2005), Baseline Surface Radiation Network (BSRN) operations manual version 2.1, *Rep. WCRP-121, WMO/TD-NO.1274*, World Clim. Res. Programme, Geneva, Switzerland.

McGuffie, K., and A. Henderson-Sellers (1985), The diurnal hysteresis of snow albedo, *J. Glaciol.*, *31*, 188–189.

Meinander, O., A. Konku, K. Lakkala, A. Heikkilä, L. Ylianttila, and M. Toikka (2008), Diurnal variations in the UV albedo of arctic snow, *Atmos. Chem. Phys.*, *8*, 6551–6563, doi:10.5194/acp-8-6551-2008.

Miller, J. C., and J. N. Miller (1993), *Statistics for Analytical Chemistry*, Ellis Horwood, Chichester, U. K.

Minnis, P., S. Mayor, W. L. Smith Jr., and D. F. Young (1997), Asysmetry in the diurnal variation of surface albedo, *IEEE Trans. Geosci. Remote Sens.*, *35*(4), 879–890, doi:10.1109/36.602530.

Oleson, K. W., G. B. Bonan, C. B. Schaaf, F. Gao, Y. Jin, and A. H. Strahler (2003), Assessment of global climate model land surface albedo using MODIS data, *Geophys. Res. Lett.*, *30*(8), 1443, doi:10.1029/2002GL016749.

Picard, D., L. Arnaud, F. Domine, and M. Fily (2009), Determining snow specific surface area from near-infrared reflectance measurements: Numerical study of the influence of grain shape, *Cold Reg. Sci. Technol.*, *56*, 10–17, doi:10.1016/j.coldregions.2008.10.001.

Pirazzini, R. (2004), Surface albedo measurements over Antarctic sites in summer, *J. Geophys. Res.*, *109*, D20118, doi:10.1029/2004JD004617.

Pirazzini, R., T. Vihma, M. A. Granskog, and B. Cheng (2006), Surface albedo measurements over sea ice in the Baltic Sea during the spring snowmelt period, *Ann. Glaciol.*, *44*, 7–14, doi:10.3189/172756406781811565.

Roesch, A. (2006), Evaluation of surface albedo and snow cover in AR4 coupled climate models, *J. Geophys. Res.*, *111*, D15111, doi:10.1029/2005JD006473.

Salomon, J. G., C. B. Schaaf, A. H. Strahler, F. Gao, and Y. Jin (2006), Validation of the MODIS bidirectional reflectance distribution function and albedo retrievals using combined observations from the Aqua and Terra platforms, *IEEE Trans. Geosci. Remote Sens.*, *44*, 1555–1565, doi:10.1109/TGRS.2006.871564.

Schaepman-Strub, G., M. E. Schaepman, T. H. Painter, S. Dangel, and J. V. Martonchik (2006), Reflectance quantities in optical remote sensing-definitions and case studies, *Remote Sens. Environ.*, *103*, 27–42, doi:10.1016/j.rse.2006.03.002.

Schwerdtfeger, P. (1976), *Physical Principles of Micrometeorological Measurements*, 113 pp., Elsevier Sci., New York.

Seckmeyer, G., A. Bais, G. Bernhard, M. Blumthaler, P. Eriksen, R. L. McKenzie, C. Roy, and M. Miyauchi (2001), Instruments to measure solar ultraviolet radiation, part I: Spectral instruments, WOM-GAW Rep. 125, World Meteorol. Org., Geneva, Switzerland.

Sommerfeld, R. A., and E. LaChapelle (1970), The classification of snow metamorphism, *J. Glaciol.*, *9*, 3–17.

Song, J. (1998), Diurnal asymmetry in surface albedo, *Agric. For. Meteorol.*, *92*, 181–189, doi:10.1016/S0168-1923(98)00095-1.

Strahler, A. H., et al. (1999), MODIS BRDF/Albedo product: Algorithm theoretical basis document version 5.0, *MODIS Prod. MOD43*, NASA Goddard Space Flight Cent., Greenbelt, Md.

Taillandier, A.-S., F. Domine, W. R. Simpson, M. Sturm, and T. A. Douglas (2007), Rate of decrease of the specific surface area of dry snow: Isothermal and temperature gradient conditions, *J. Geophys. Res.*, *112*, F03003, doi:10.1029/2006JF000514.

Wang, X., and C. S. Zender (2010a), MODIS albedo bias at high zenith angle relative to theory and to in situ observations in Greenland, *Remote Sens. Environ.*, *114*, 563–575, doi:10.1016/j.rse.2009.10.014.

Wang, X., and C. S. Zender (2010b), Constraining MODIS snow albedo bias at large solar zenith angles: Implications for surface energy budget in Greenland, *J. Geophys. Res.*, *115*, F04015, doi:10.1029/2009JF001436.

Wang, Z., M. Barlage, X. Zeng, R. E. Dickinson, and C. B. Schaaf (2005), The solar zenith angle dependence of desert albedo, *Geophys. Res. Lett.*, *32*, L05403, doi:10.1029/2004GL021835.

Warren, S. G. (1982), Optical properties of snow, *Rev. Geophys. Space Phys.*, *20*, 67–89, doi:10.1029/RG020i001p00067.

Warren, S. G., and W. J. Wiscombe (1980), A model for the spectral albedo of snow. II: Snow containing atmospheric aerosols, *J. Atmos. Sci.*, *37*, 2734–2745, doi:10.1175/1520-0469(1980)037<2734:AMFTSA>2.0.CO;2.

Warren, S. G., R. E. Brandt, and P. O. Hinton (1998), Effect of surface roughness on bidirectional reflectance of Antarctic snow, *J. Geophys. Res.*, *103*, 25,789–25,807, doi:10.1029/98JE01898.

Weller, G. E. (1969), Radiation diffusion in Antarctic ice media, *Nature*, *221*, 355–356, doi:10.1038/221355a0.

Winther, J.-G., F. Godtliebsen, S. Gerland, and P. E. Isachsen (2002), Surface albedo in Ny-Ålesund, Svalbard: Variability and trends during 1981–1997, *Global Planet. Change*, *32*, 127–139, doi:10.1016/S0921-8181(01)00103-5.

Wiscombe, W. J., and S. G. Warren (1980), A model for the spectral albedo of snow. I: Pure snow, *J. Atmos. Sci.*, *37*, 2712–2733, doi:10.1175/1520-0469(1980)037<2712:AMFTSA>2.0.CO;2.

Wuttke, S. (2005), Radiation conditions in an Antarctic environment, *Ber. Polarforsch. Meeresforsch.*, *514*, 148 pp.

Wuttke, S., G. Seckmeyer, and G. Kőnig-Lango (2006), Measurements of spectral snow albedo at Neumayer, Antarctica, *Ann. Geophys.*, *24*, 7–21, doi:10.5194/angeo-24-7-2006.

X. Wang, School of Geography and Planning, Sun Yat-sen University, 135 Xingang West Rd., Guangzhou, Guangdong 510275, China. (wangxw8@mail.sysu.edu.cn)

C. S. Zender, Department of Earth System Science, University of California, 3323 Croul Hall, Irvine, CA 92697-3100, USA.